ARTICLE

The impact of stromal Hic-5 on the tumorigenesis of colorectal cancer through lysyl oxidase induction and stromal remodeling

Tomokatsu Omoto[1] · Joo-ri Kim-Kaneyama[1] · Xiao-Feng Lei[1] · Akira Orimo[2] · Koji Ohnishi[3] · Kosuke Yoshihara[4] ·
Aya Miyauchi[1] · Shuo Li[1] · Lin Gao[1] · Takahiro Umemoto[5] · Junichi Tanaka[5] · Kenta Nakahara[6] · Motohiro Takeya[3] ·
Fumio Ishida[6] · Shin-ei Kudo[6] · Shogo Haraguchi[1] · Takuro Miyazaki[1] · Akira Miyazaki[1]

Abstract

Carcinoma-associated fibroblasts (CAFs) influence tumor initiation, progression, and metastasis within the tumor-associated stroma. This suggests that CAFs would be a potential target for tumor therapy. Here we found that Hydrogen peroxide-inducible clone-5 (Hic-5), also named transforming growth factor beta-1-induced transcript 1 protein (Tgfb1i1), was strongly induced in CAFs found in human colorectal cancer. To investigate the role of Hic-5 in CAFs, we isolated CAFs and the control counterpart normal fibroblasts (NFs) from human colorectal cancer and non-cancerous regions, respectively. Hic-5 was highly expressed in isolated human CAFs and strongly induced in NFs in culture by the supernatant from cultured colorectal cancer cells as well as cytokines such as TGF-β, IL-1β and stromal cell-derived factor 1 (SDF-1/CXCL12). Furthermore, tumor growth was inhibited in a co-culture assay with Hic-5 knockdown fibroblasts compared with control fibroblasts. To clarify the function and significance of Hic-5 in colorectal cancer in vivo, we utilized a mouse model of azoxymethane (AOM)-induced colorectal cancer using Hic-5-deficient mice. Lack of Hic-5 in CAFs completely prevented AOM-induced colorectal cancer development in the colon tissues of mice. Mechanistic investigation revealed that Hic-5 promoted the expression of lysyl oxidase and collagen I in human control counterpart fibroblasts. Taken together, these results demonstrate that Hic-5 in CAFs is responsible for orchestrating or generating a tumor-promoting stroma.

✉ Joo-ri Kim-Kaneyama
 shuri@pharm.showa-u.ac.jp

[1] Department of Biochemistry, Showa University School of Medicine, Tokyo, Japan

[2] Department of Pathology and Oncology, Juntendo University School of Medicine, Tokyo, Japan

[3] Department of Cell Pathology, Graduate School of Medical Sciences, Faculty of Life Sciences, Kumamoto University, Kumamoto, Japan

[4] Department of Obstetrics and Gynecology, Niigata University Graduate School of Medical and Dental Sciences, Niigata, Japan

[5] Department of Gastroenterological and General Surgery, Showa University Fujigaoka Hospital, Yokohama, Japan

[6] Digestive Disease Center, Showa University Northern Yokohama Hospital, Tsuzuki-ku, Yokohama, Japan

Introduction

Extracellular matrix (ECM) remodeling in the tumor stroma is one of the essential events for cancer development and progression. Clinically, tumors are often found to be stiffer than the surrounding tissue and the increased stiffness of the tumor environment is known to regulate tumor malignancy by enhancing integrin-dependent mechanotransduction [1, 2]. Interestingly, breast cancer cells can be reverted into phenotypically normal cells by manipulating the environmental context [3]. There is increasing evidence that cancer development can be controlled by the ECM remodeling enzymes such as matrix metalloproteinases, hyaluronan synthases and lysyl oxidase (LOX). LOX is a secreted copper-dependent amine oxidase, which exclusively catalyzes the cross-linking of collagens and elastin through oxidative deamination of lysine residues [4, 5]. The secreted LOX has been shown to increase ECM stiffness, activate

oncogenic signaling pathways and play a tumor-promoting role through ECM remodeling [6, 7]. Previous work by Levental et al. identified that stroma-derived LOX is one of the key mediators promoting tumorigenesis, and tumor-associated stroma has been recognized as a potential therapeutic target against tumors [8].

Hydrogen peroxide-inducible clone-5 (Hic-5), is a scaffold protein that shuttles between the nucleus and the focal adhesion complex [9]. Previous studies have demonstrated that Hic-5 plays key roles in the pathogenesis of various disorders such as liver fibrosis, atherosclerosis, aneurysm, glomerulonephritis, wound healing, and prostate cancer [10–15]. Mechanistic investigations of these studies showed that Hic-5 was responsible for regulating the organization of ECM as both a mechanical stress responsible mobile adaptor and transcriptional co-factor. In this study, we test the hypothesis that stromal Hic-5 expression contributes to colorectal carcinoma (CRC) development. We first examined Hic-5 expression in the tissues from human CRC. In addition, we investigated the mechanisms by which stromal Hic-5 contributes to development of CRC. Finally, we demonstrated that Hic-5 serves as a key regulator in the CRC development using Hic-5 knockout mice.

Results

Hic-5 expression was induced in human CRC, especially in CAFs of the tumor stroma

We first assessed Hic-5 expression in normal human colon mucosa and human CRC. Real-time reverse transcriptase polymerase chain reaction (RT-PCR) and western blot analyses showed that Hic-5 expression levels of mRNA and protein were markedly increased in human CRC compared to those of normal human colon mucosa (Fig. 1a, b). Hence, we analyzed Hic-5 expression by immunohistochemistry in normal human colon mucosa, colorectal adenoma and carcinoma. We found that Hic-5 was expressed in the stromal compartment of all CRC samples whereas only slightly expressed in the resident fibroblasts in normal colon mucosa (Fig. 1c). Then, we evaluated the levels of Hic-5 expression in colorectal adenoma and carcinoma; two pathologists scored normal colon mucosa, colorectal adenoma and carcinoma according to the degree of Hic-5 expression. This result indicated that Hic-5 expression was significantly increased in carcinoma (Fig. 1d).

To evaluate the reliability of Hic-5 expression in the stromal compartment of CRC, we correlated stromal score values generated using the ESTIMATE algorithm with Hic-5 expression. Remarkably, Hic-5 expression was positively correlated with the ESTIMATE-based stromal scores derived from four independent CRC data sets (The

cancer genome atlas (TCGA) COAD READ, Gene Expression Omnibus (GEO), GSE14333, GSE33113 and GSE39582) (Fig. 2a). Similarly, we found that Hic-5 was highly expressed in stroma than epithelium using two GEO data sets (GSE35602 and GSE39395), in which the cells were separated by microdissected or fluorescence-activated cell sorting, respectively (Fig. 2b). These results confirmed the stromal-specific expression of Hic-5 in comparison to the cancerous epithelial expression. Subsequently, we analyzed colocalization of Hic-5 with each of the following proteins, α-SMA, CD31, CD45 and Iba1; the cell type markers for activated fibroblasts, endothelial cells, lymphocytes and macrophages, respectively. Co-immunostaining of human CRC tissues with antibodies against Hic-5 and each cell type marker revealed that Hic-5 was highly expressed in CAFs in addition to lower expression in endothelial cells (Fig. 3a). In contrast, neither lymphocytes nor macrophages expressed Hic-5 (Fig. 3a). These results indicated that Hic-5 was most commonly expressed in CAFs in CRC. It is noteworthy that Hic-5 is dominantly expressed in CAFs adjacent to epithelial cancer cells within many parts of cancer stroma (Fig. 3b, c, arrows).

Cancer cell-derived soluble factors induced Hic-5 expression in normal human fibroblasts

To investigate if Hic-5 is related to the activation process of fibroblasts in vitro, we isolated NFs and paired CAFs from human normal colon mucosa and CRC tissues obtained from the patients who underwent surgical resection. At first, we comparatively analyzed the expression of Hic-5 and α-SMA, an activation marker of fibroblasts, in cultured NFs and CAFs by western blot analysis. Similar to immunohistochemical analysis of human tissues, Hic-5 and α-SMA expression was significantly increased in CAFs (Fig. 4a). Immunofluorescence analysis also showed that Hic-5 expression was higher in CAFs than in NFs and detected mainly at the focal adhesion of each cell (Fig. 4b). Then we investigated how Hic-5 expression was induced in fibroblasts under the influence of cancer cells. For this purpose, we used NFs that expressed a lower level of Hic-5 than CAFs. First, we co-cultured NFs with the human colon cancer cell line, Caco-2 and analyzed Hic-5 expression by western blot analysis. Compared with culturing NFs alone, Hic-5 expression in the co-culture of NFs and Caco-2 was augmented. Conversely, Caco-2 culture showed little expression of Hic-5 (Fig. 4c). Immunocytochemical studies showed that Hic-5 expression was strongly induced in the NFs adjacent to Caco-2 (Fig. 4d). Furthermore, western blot analysis showed that Hic-5 expression was increased in NFs stimulated by the conditioned medium obtained from Caco-2 (CM^{Caco-2})
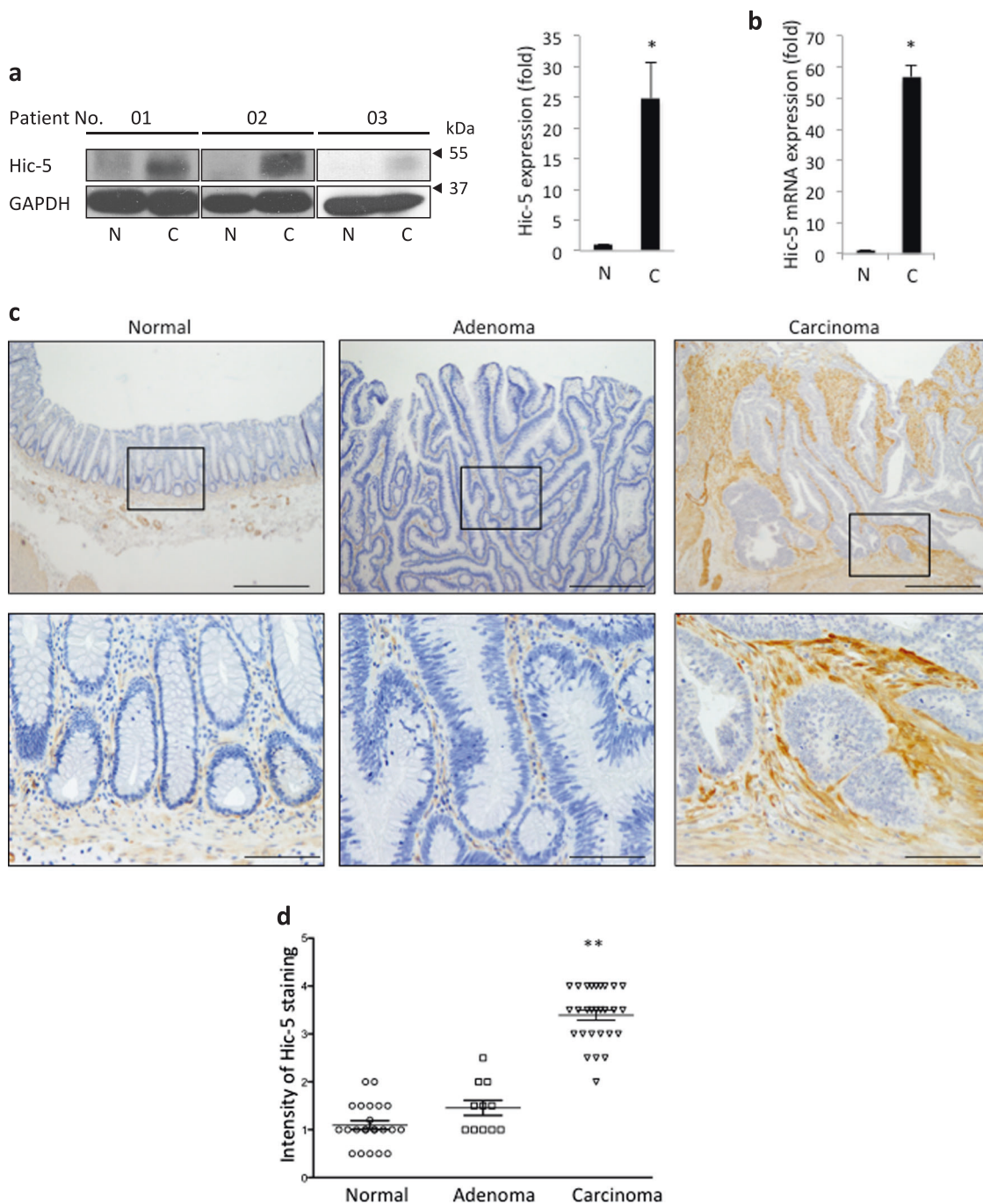
Fig. 1 Hic-5 is expressed in human colorectal cancer stroma. **a** Hic-5 protein expression in human CRC (C) and adjacent normal tissues (N) from three patients who have advanced CRCs. Expression of Hic-5 was quantified by densitometry and normalized to the corresponding signal for GAPDH ($n = 3$). **b** Quantitative RT-PCR analysis of Hic-5 expression in human CRC and adjacent normal tissues ($n = 3$). **c** Representative images of Hic-5 staining in normal human colon mucosa, adenoma and cancer tissues. Scale bars indicate 500 μm (upper panels), 100 μm (lower panels). **d** Intensity of Hic-5 staining was scored from 0 to 4. Graph representing the average intensity of Hic-5 staining for normal colon, colon adenoma and colon carcinoma. $n = 21$ (Normal), 11 (Adenoma) and 28 (Carcinoma). Two pathologists performed scoring for each slide. $*P < 0.01$, $**P < 0.05$

(Fig. 4e). In addition, cancer-related cytokines such as TGF-β, PDGF, IL-1β and SDF-1 induced Hic-5 in NFs, in which TGF-β showed the strongest effect (Fig. 4f). Of note, Hic-5 induction by these cytokines was significantly affected by treatment with SB431542 or LY364947, which are inhibitors of TGFβ signaling, indicating that Hic-5 expression by various cytokines was mediated by the TGF-β signaling (Supplementary Fig. 1a).
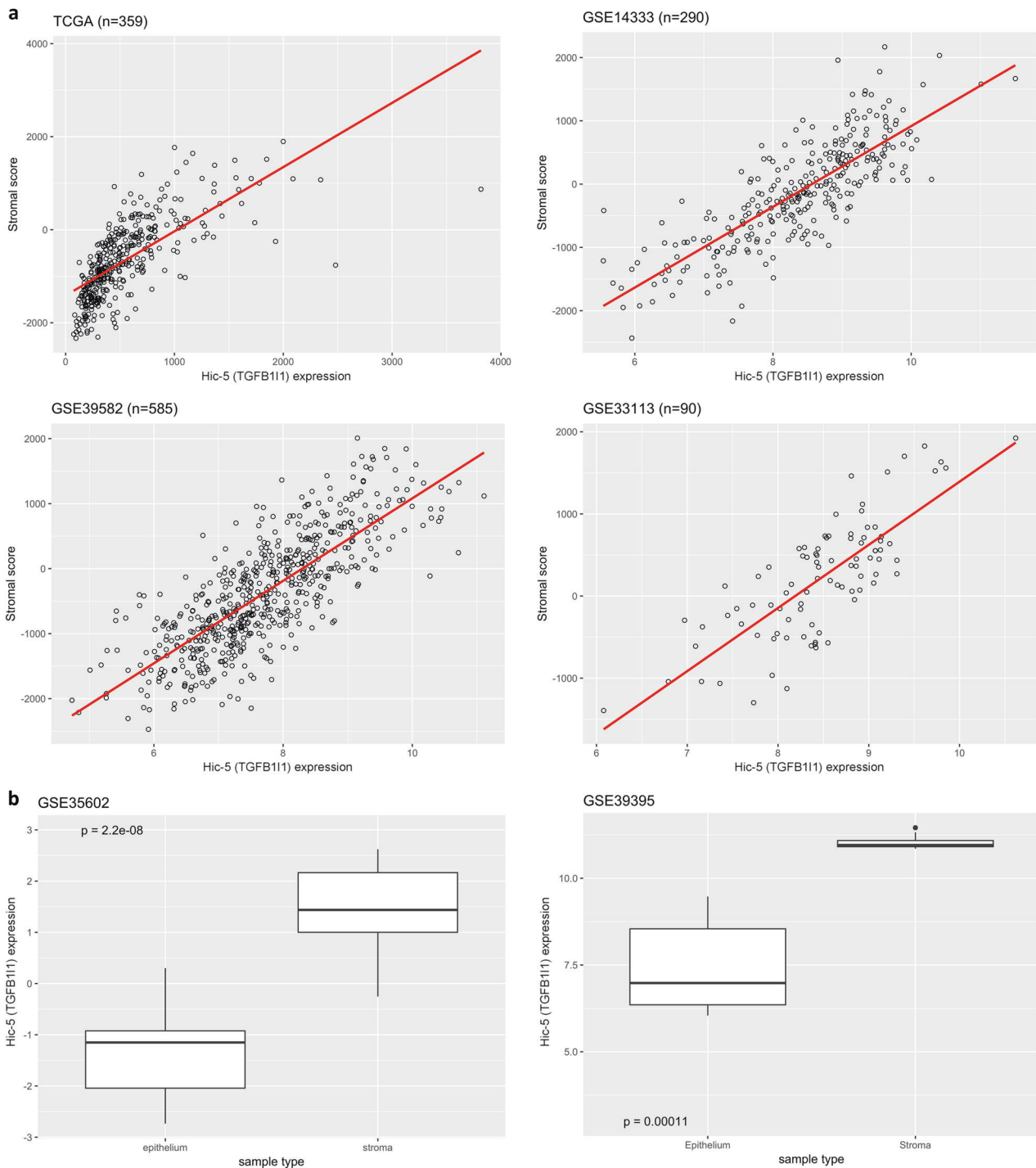
Fig. 2 Hic-5 expression is elevated in the stroma of human CRC. **a** Correlation of stroma scores obtained using the ESTIMATE algorithm with Hic-5 expression. The ESTIMATE-based stromal scores were derived from TCGA COAD, READ (Pearson r = 0.70), GSE14333 (Pearson r = 0.81), GSE33113 (Pearson r = 0.78) and GSE39582 (Pearson r = 0.79). **b** Box and whisker plots display increased Hic-5 scores for the stroma samples compared with the matched epithelium samples. GSE35602 and GSE39395 datas ets include gene expression data of epithelium and stroma isolated from colon cancer tissue using laser-micro dissection or flow cytometry, respectively
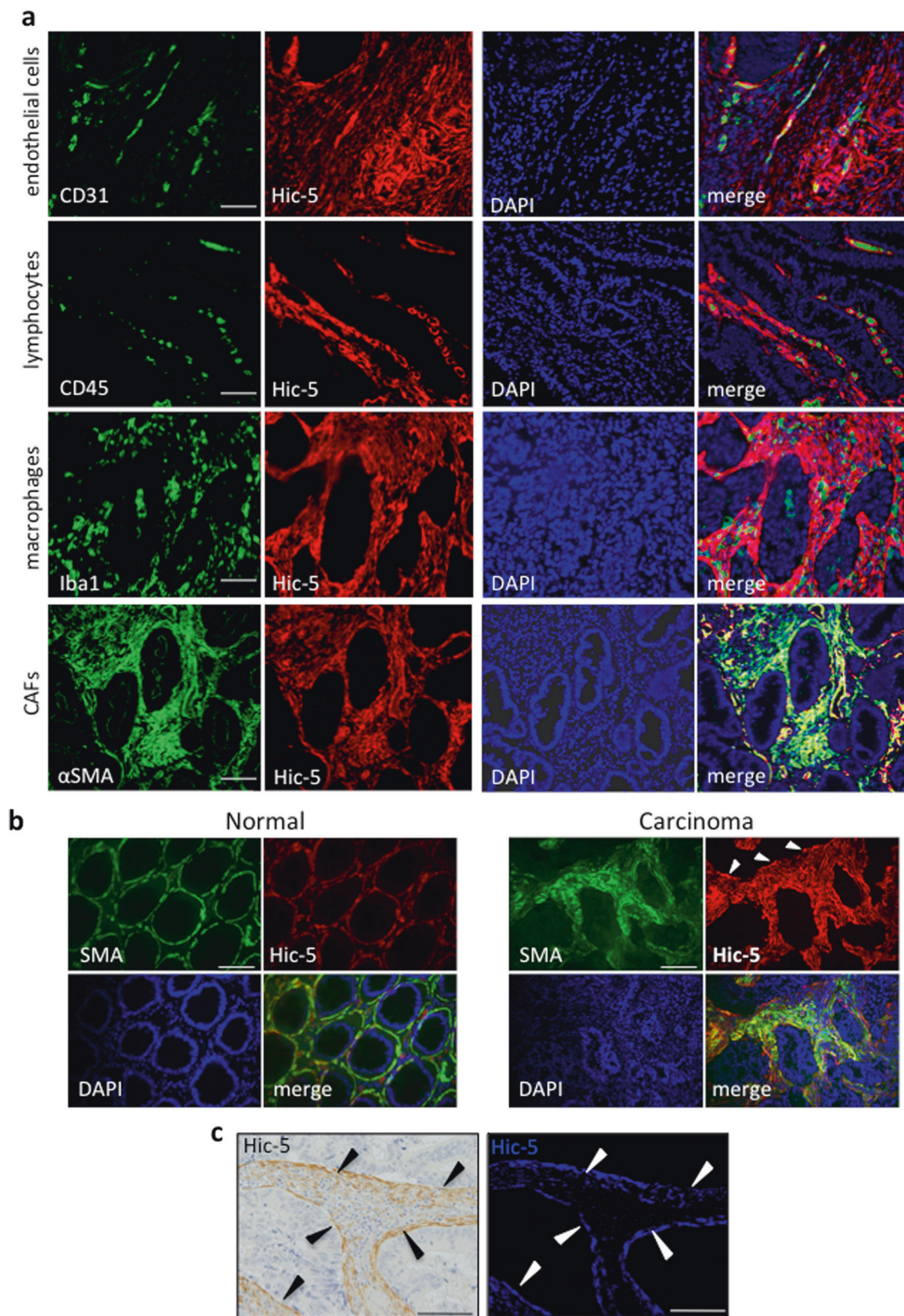
Fig. 3 Hic-5 is highly expressed in CAFs of human colorectal cancer stroma. **a** Representative image of double immunofluorescence staining for Hic-5 (red) with each of CD31 (green), CD45 (green), Iba1 (green) or α-SMA (green) in colon cancer. Scale bars indicate 50 μm. **b** Comparison of Hic-5 staining in normal mucosa and colon cancer. Arrowheads indicate the stromal cells adjacent to the cancer cells. Scale bars indicate 50 μm. Representative image of Hic-5 staining, especially expressed in CAFs adjacent to epithelial cancer cells was indicated in **c**. Hic-5 positive area in left panel was highlighted blue with Lumina vision software in right panel. Scale bars indicate 100 μm

a

b

c

d

e

d
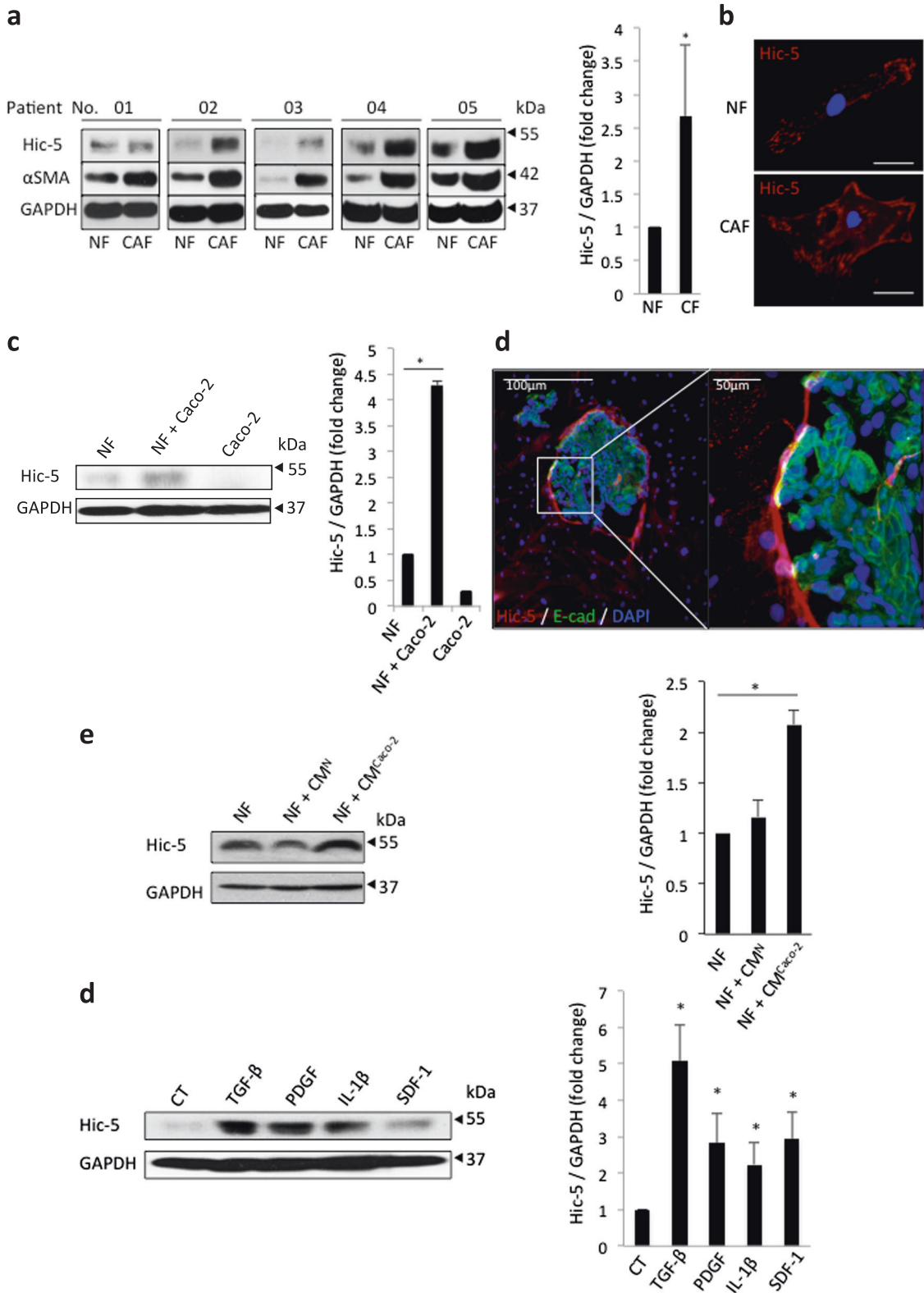
◀ **Fig. 4** Hic-5 expression was increased in NFs by cancer-related cytokines and cancer cell-derived culture media. **a** Western blot for Hic-5 in normal human fibroblasts (NFs) and human cancer-associated fibroblasts (CAFs) derived from patient tissues. The right graph shows quantitative analyses of Hic-5 expression after normalization with GAPDH ($n = 8$). **b** Representative immunofluorescence staining for Hic-5 in cultured NFs (upper) and CAFs (lower) from patients. Scale bars indicate 25 μm. **c** Hic-5 expressions in cultured NFs, Caco-2 and a co-culture of NFs and Caco-2. The right graph shows quantitative analysis of Hic-5 expression after normalization with GAPDH ($n = 4$). **d** Representative double immunofluorescence staining for Hic-5 (red) and E-cadherin (green) in co-cultured NFs and Caco-2. **e** Hic-5 expression in NFs which were stimulated by conditioned media from Caco-2 or normal colonic epithelial cells. Quantitative analysis of Hic-5 is shown in the right graph ($n = 4$). *$P < 0.01$. **f** Hic-5 expression in NFs that was stimulated by TGF-β, PDGF, IL-1β or SDF-1, respectively. Quantitative analyses of Hic-5 is shown in the right graph ($n = 4$). *$P < 0.05$

## Stromal Hic-5 regulates LOX expression and cancer cell proliferation

As Hic-5 was expressed in stromal cells in CRC, we next attempted to investigate its effects on the tumor-stroma interactions. For this purpose, we established Hic-5 repressed NFs (NFs/shHic-5) by using short hairpin RNA (shRNA) for Hic-5. We evaluated the influence of Hic-5 on the growth of Caco-2 in a co-culture assay. The areas of Caco-2 colonies were suppressed significantly in co-culturing with NFs/shHic-5 (Fig. 5a). Expression of E-cadherin was used to substantiate epithelial phenotype in the carcinoma cell lines. This result indicates that Hic-5 in stromal fibroblasts could promote tumor progression in the carcinoma-microenvironment. To investigate the contributing roles of Hic-5 in the carcinoma-microenvironment, we evaluated LOX, one of the important regulators of extracellular matrix and collagen I expression. Compared to the upregulation of LOX and collagen I expression in wild-type NFs (NFs/WT) adjacent to Caco-2, their expression was suppressed in NFs/shHic-5 (Fig. 5b). Under the circumstances tested, Hic-5 was not induced in the Hic-5 knocked down NFs even by co-culture with Caco-2 (Supplementary Fig. 1c). Furthermore, we overexpressed Hic-5 in NFs/WT through adenovirus-mediated gene transfer and compared it with the control gene. Western blot analysis indicated exogenous Hic-5 induced LOX expression in NFs/WT (Fig. 5c). RT-PCR analysis also showed that collagen I (Col1a1) gene was significantly upregulated in Hic-5 overexpressed NFs/WT (Fig. 5d). Following this, we investigated LOX and Collagen I expression in NFs/shHic-5. Western blot analysis showed that LOX levels were significantly increased after TGF-β treatment in NFs/WT but not in NFs/shHic-5 (Fig. 5e). RT-PCR analysis confirmed that collagen I (Col1a1) gene was significantly upregulated in WT/NF (Fig. 5f).

Nuclear Hic-5 induced the expression of LOX

We proceeded to investigate how Hic-5 induced LOX expression in NFs. Hic-5 was stained in smooth muscle as well as in CAFs in human tissue. As the result, whole cytoplasm was stained in smooth muscle (Fig. 6a, left), but in CAFs and it was strongly expressed in the nucleus particularly in the areas adjacent to cancer cells (Fig. 6a, right). In addition, immunofluorescent analysis showed TGF-β stimulation induced Hic-5 accumulation in the nucleus of NFs (Fig. 6b, left panel). It was more prominent in the presence of Leptomycin B, an inhibitor for nuclear export (Fig. 6b, right panel). Based on these results, we examined LOX expression under the condition that Hic-5 was forcibly expressed in cytoplasm or in nucleus of NFs/shHic-5. Immunofluorescent analysis showed the LOX expression. As expected, Hic-5 with NLS (+NLS-Hic-5) was localized in the nuclei as visualized with anti-HA (Fig. 6c, lower panel) and could promote LOX transcriptional activity in NFs /shHic-5 (Fig. 6d, lower panel). In contrast, Hic-5 without NLS (−NLS-Hic-5), which remained almost in the cytoplasm, could not stimulate LOX transcriptional activity even when overexpressed (Figs. 6c, d, upper panels). Western blot analysis also indicated that LOX levels were significantly increased in +NLS-Hic-5 expressed NFs, but not in −NLS-Hic-5 expressed NFs (Fig. 6e).

Reduction in azoxymethane (AOM)-induced colonic tumorigenesis in Hic-5 knockout mice

As with human tissues, double-immunofluorescent staining analysis indicated that Hic-5 expression overlapped with α-SMA positive cells as seen by the yellow fluorescence in the stromal cells of normal colon mucosa and colon cancer in mice (Fig. 7a). This finding reinforced the notion that Hic-5 was expressed restrictedly in CAFs but not in carcinoma cells in AOM-induced colon cancers as well as human CRC. To investigate roles of stromal Hic-5 expression on carcinogenesis, Hic-5 KO mice, which we generated previously [16], and the age- and sex-matched wild-type mice were injected with AOM (Fig. 7b). Wild-type mice treated with AOM developed tumors mainly located in the distal part of the colon (Fig. 7c, left panel). In contrast, no tumor was observed with Hic-5 KO mice until 20 weeks after AOM administration (Fig. 7c and Table 1) and hyperplastic polyp was found only in one place at 24 weeks (data not shown). Hence, there was a difference in the proportion of colon weight to body weight of the wild-type mice compared to that of the Hic-5 KO mice (Fig. 7d). Histological examination also revealed that advanced adenocarcinoma occurred only in the wild-type mice after AOM treatment (Figs. 7a, e, left panels). There was no, histological
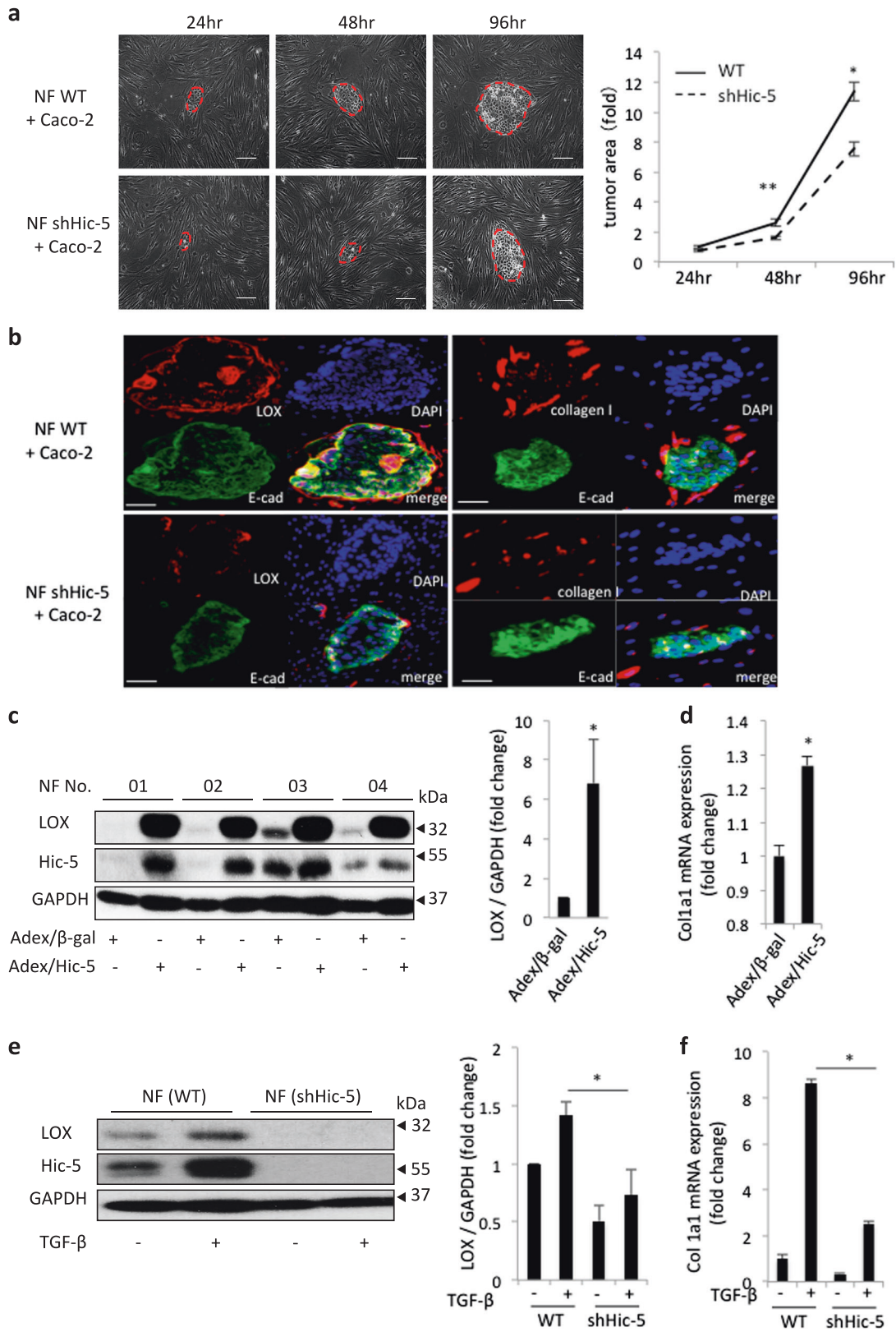
◀ **Fig. 5** **a** Representative image of Caco-2 colony co-cultured with NFs as a control or with NF transfected and cloned with Hic-5 shRNA (NF/shHic-5). Quantitative analyses of Caco-2 areas are shown in the right graph ($n = 3$). Scale bars indicate 100 μm. **b** Representative double immunofluorescence staining images for LOX or collagen I (red) with E-cadherin (green) in co-cultured Caco-2 with NFs as a control or with NF/shHic-5. Scale bars indicate 100 μm. **c**, **d** Western blot analysis of LOX and Hic-5 (**c**) and mRNA expression of collagen I (**d**) in cultured NFs. Cells were infected with adenovirus-mediated flag-tagged Hic-5 (Ad-Hic-5/flag) or β-galactosidase (Ad/ β-gal) as a control for 72 h ($n = 4$). **e**, **f** Western blot analysis of LOX and Hic-5 (**e**) and mRNA expression of collagen I (**f**) in cultured NFs as a control or in NF/shHic-5. These cells were treated with TGF- β1 (5 ng/ml) for 24 h. The result of quantitative analyses is shown in right graphs ($n = 4$). *$P < 0.01$, **$P < 0.05$

evidence for carcinoma development in Hic-5 KO mice (Figs. 7a, e right panels).

Discussion

In this study, we identified Hic-5 in CAFs as a novel factor responsible for the development of CRC through ECM remodeling. To our knowledge, Hic-5 is the first reported non-enzymatic adaptor protein regulating the carcinogenesis of CRC via profound tissue remodeling processes by CAFs.

CRC is one of the most intensively studied cancer types and the morphological steps in the adenoma-carcinoma sequence have been elucidated. The Fearon- Vogelstein adenoma carcinoma multistep model centers on the genetic changes such as tumor suppressor genes (*APC, TP53, SMAD2, SMAD4 and p16INK4a*), proto-oncogenes (*K-ras, N-ras*) and DNA repair genes (*MMR and MUTYH*) [17]. On the other hand, recent studies have shown that the stromal extracellular matrix and CAFs contribute to the development of a wide variety of tumors [18–23]. In particular, Orimo and Weinberg et al. substantiated that CAFs in human breast carcinomas enhanced tumor growth and angiogenesis [21]. In the present study, mice lacking Hic-5 in CAFs dramatically attenuated AOM-induced colorectal cancer in vivo, indicating that Hic-5, specifically expressed in CAFs but not in cancer cells, is responsible for carcinogenesis. Interestingly, Hic-5 expression within the carcinoma in the adenoma was modest, whereas Hic-5 is highly expressed in the stroma of all of advanced carcinoma tissues (data not shown). This result suggests that Hic-5 expression levels in stroma are associated with the potential for malignant transformation. In this regard, it is noteworthy that fibroblast-specific deletion of Hic-5 in mice would reveal Hic-5 function in CAFs more concisely. Furthermore, Hic-5 expression was previously reported in breast, prostate, colon and liver cancer, albeit that these studies were focused on Hic-5 function in cancer cells themselves [24–27]. However, a recent study, using mouse CAFs shows that Hic-5 expression in the stroma is required for breast cancer cell growth in mice [28]. Moreover, this effect is characterized by the matrix deposition by Hic-5 in mouse CAFs surrounding breast cancer cells. Actually, the elaborate architectures in tissues are maintained by a dynamic equilibrium between the synthesis and the degradation of the ECM. However, along with tumor growth, this dynamic equilibrium is broken and abnormal *ECM* leads to a stiff matrix and affects cancer progression. It is also known that altering the proper balance of ECM signal induces cancer development and progression [29]. In this study, we also demonstrate that Hic-5 was dominantly expressed in human CAFs adjacent to epithelial cancer cells and its expression was strongly induced in the NFs adjacent to Caco-2 (Fig. 4d). In addition, Hic-5 silenced CAFs could not induce LOX and collagen I expression even though heterotypic signaling by cancer-stroma direct interaction existed in the co-culture assay. At the same time, Hic-5 silenced stromal CAFs could suppress cancer cell growth. These data establish Hic-5 as a key player in colorectal carcinogenesis by promoting production of ECM and collagen cross-linker LOX that lead to stiffness of cancer tissues (Fig. 8).

We and others previously reported that Hic-5 deficiency attenuates fibrotic diseases such as liver fibrosis, aortic aneurysm and scar formation [10, 12, 30]. The common phenomenon of these diseases is accompanied by increases in tissue stiffness, loss of elasticity and probably inappropriate post-translational cross-linking of ECM proteins. According to an analysis of previous studies, Hic-5 links various intracellular signaling modules by coordinating multiple protein-protein interactions at the focal adhesions and in the nucleus. Considering that Hic-5 is a TGF-β-, reactive oxygen species- and mechanical force-sensitive mobile scaffold molecule between focal adhesions, stress fibers and the nucleus, it is reasonable to assume that Hic-5 might form various reaction fields by providing itself as a scaffold for reactive sites throughout the cell.

Hic-5 was originally isolated as a TGF-β-inducible gene and can shuttle between focal adhesions and the nucleus, suggesting a possible role in carrying cytoplasmic signals into the nucleus [9]. Intriguingly, the nuclear accumulation of Hic-5 is more clearly observed in the surrounding parts of the cancer cells compared to other parts of the tissue. We also found that TGF-β enhanced the nuclear accumulation of Hic-5 in cultured human NFs, and the nuclear accumulation of Hic-5 induced LOX expression. It is well known that LOX enhances tumor progression by remodeling the tumor microenvironment [31]. TGF-β1 is also reportedly involved in the regulation of LOX expression via the activation of Smad3 and mitogen-activated protein kinase signaling [32]. Hic-5 could be regarded as a regulator involving in these signaling or bind some transcription factors such as SP1 and PPARγ, for LOX expression.
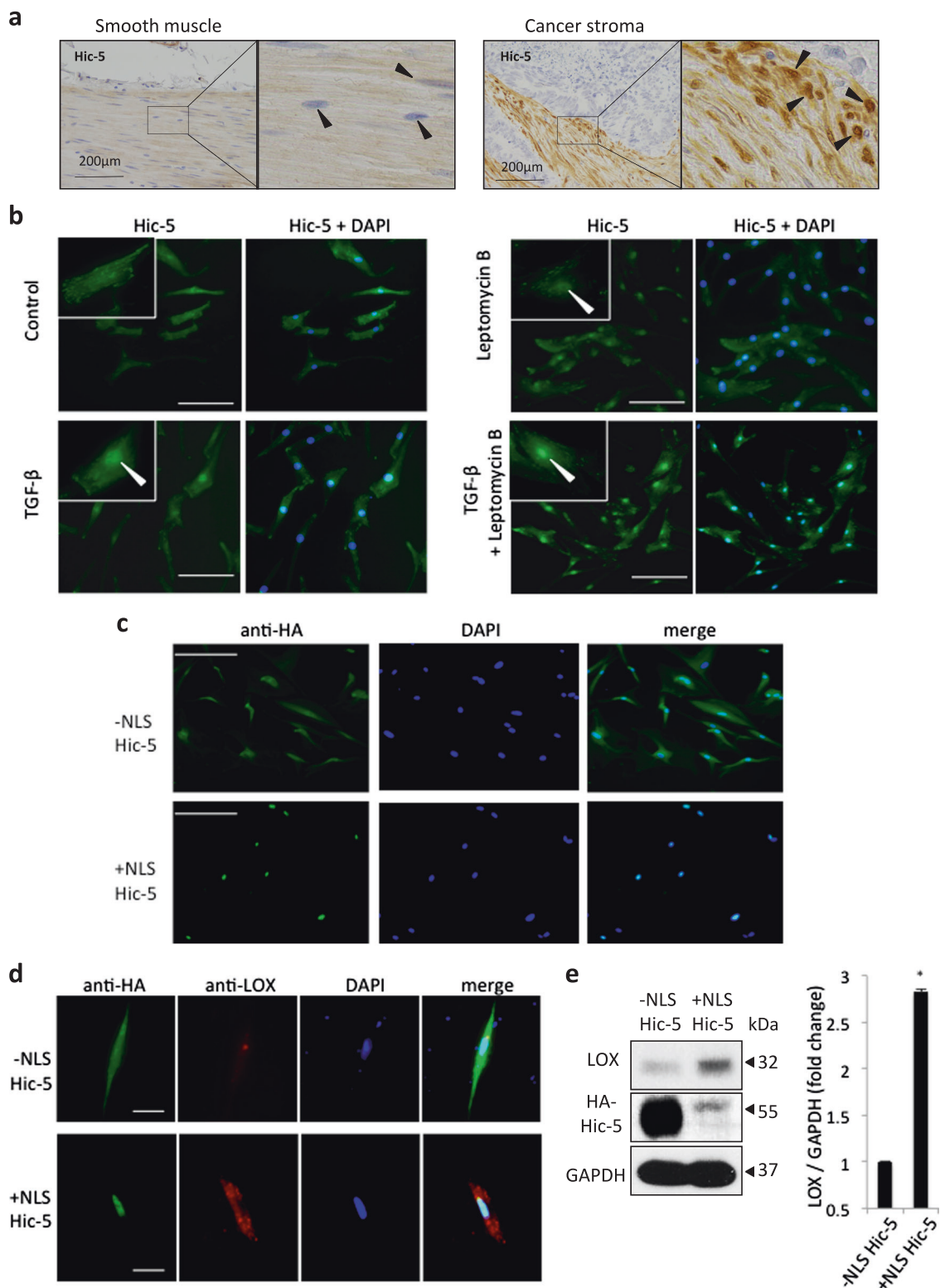
Fig. 6 Nuclear localized Hic-5 induced the expression of LOX. **a** Representative images of Hic-5 staining in smooth muscle (left panel) and cancer stroma (right panel). Arrowheads indicate nucleus. **b** Immunofluorescence staining for Hic-5 in cultured NFs with or without TGF-β (left panels) and under Leptomycin B (right panels). Scale bars indicate 100 μm. **c** Immunofluorescence staining for exogenously expressed HA-Hic-5 in cultured NFs. Scale bars indicate 100 μm. **d** Double immunofluorescence staining for HA (green) and LOX (red) in cultured NFs transfected with NLS− or NLS + Hic-5 expression vectors. Scale bars indicate 25 μm. **e** Western blot for transfected NLS− or NLS + HA-Hic-5 and LOX, and quantification of the relative level of LOX. *$P < 0.01$
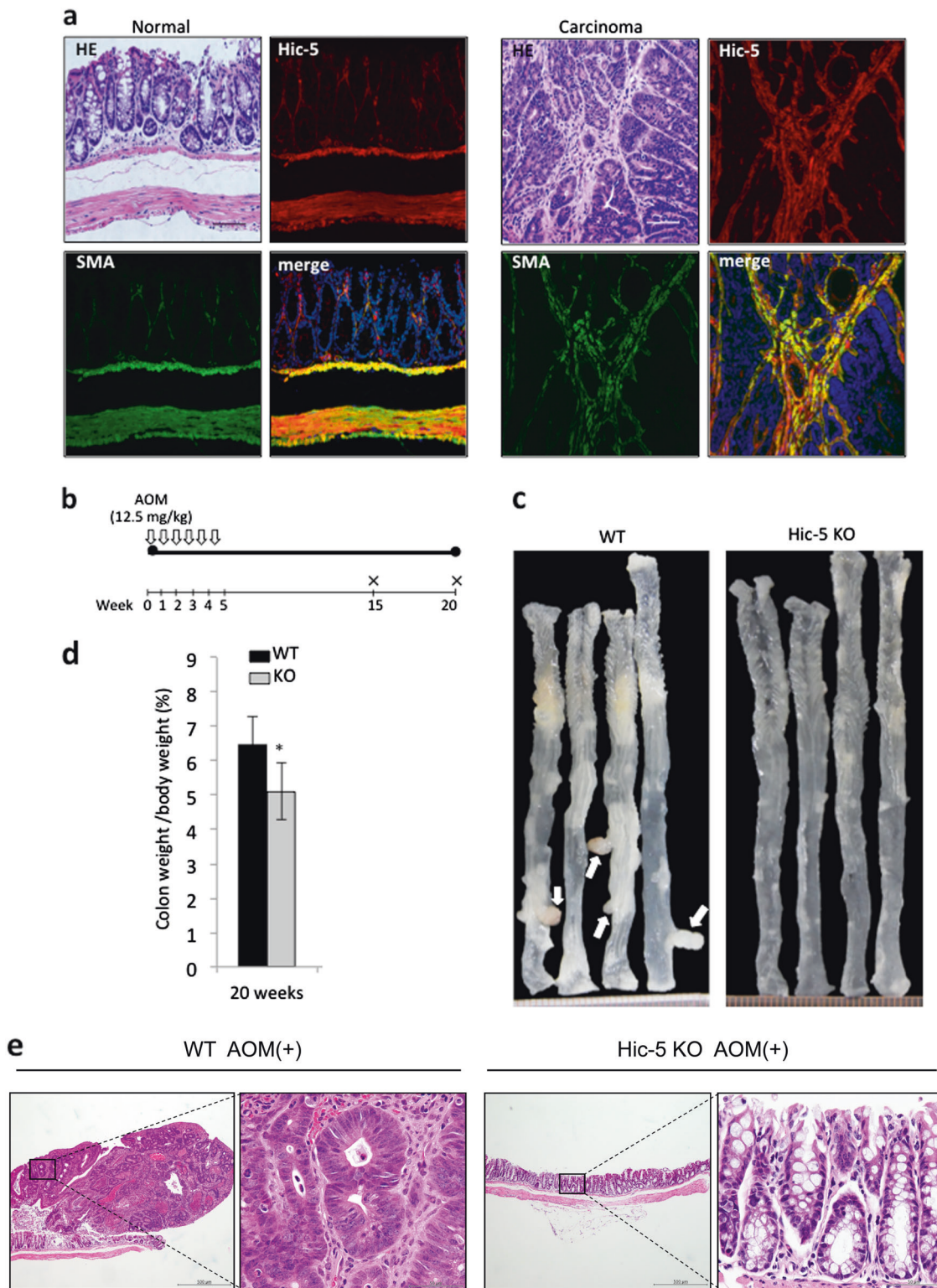
Fig. 7 Hic-5 deficiency dramatically decreased the development of colorectal cancer in mice **a**. Hematoxylin and eosin (HE) and immunofluorescence staining for Hic-5 (red) and a-SMA (green) in noncancerous mucosa (left) and colon cancer (right) in AOM-induced WT mice colon. Scale bars indicate 100 μm. **b** Timeline of the experimental procedure. Azoxymethane (AOM) was intraperitoneally injected with an amount of 12.5 mg/kg (weight) once a week for 6 weeks in a row. **d** The proportion of the weight of colon at 20 weeks after AOM treatment. WT ($n = 19$) and Hic-5 KO ($n = 17$) mice were used. **c** Representative image of colon for 20 weeks after AOM treatment. **e** HE staining in AOM treated colon at WT (left) and Hic-5 KO (right) mice. Scale bars indicate 500 μm (left panels), 50 μm (right panels)

Table 1 Tumor incidence after AOM treatment in WT and Hic-5 knockout mice

Group	Tumor incidence
15-week	
Wild type ($n = 5$)	40.0 (2/5)
Hic-5 knockout ($n = 5$)	0.0 (0/5)
P value	1.000
20-week	
Wild type ($n = 11$)	55.0 (6/11)
Hic-5 knockout ($n = 8$)	0.0 (0/8)
P value	0.018[*]

Values are presented as % (number/subtotal)

*Statistical significance between wild type and Hic-5 knockout group ($P < 0.05$). Fisher's exact test

In summary, our study identifies a key role for Hic-5 in tumor malignancy by providing a tumor-promoting microenvironment. In other words, this study found that this adaptor molecule in CAFs regulates the development of CRC via the control of its microenvironment. This supports emerging findings that targeting stromal ECM composition may be valid for future therapeutic approaches.

Materials and methods

Isolation of NFs and CAFs from human tissues

Tissue specimens were obtained with informed patient consent as approved by the Research Ethics Board (Showa University). To isolate the normal fibroblasts (NFs) and CAFs, normal mucosa and CRC were cut and minced using a scissors. Tissues were digested with collagenase A (1.5 mg/ml; Roche) at 37 °C with agitation for 60 min in Dulbecco's Modified Eagle's Medium (DMEM; WAKO Chemicals) with 10% fetal bovine serum (FBS) in a 5% CO_2-humidified atmosphere. NFs and CAFs grew around the explants and were cultured for approximately 3 weeks. Then, tissue fragments were removed, cells were trypsinized and seeded at 70–90% confluence and cultured in complete medium. After that, the NFs were immortalized using Lenti-hTERT Virus Cell Immortalization Reagent (Applied Biological Materials) following the manufacturer's protocol. Next, short hairpin RNA (shRNA) technology was used for gene silencing. NFs were stably transfected with shRNA targeting Hic-5 using shRNA (h) Lentiviral Particles (Santa Cruz) following the manufacturer's protocol. This lentiviral product included a pool of concentrated viral particles containing 3 target-specific constructs to knock down Hic-5 gene expression. Puromycin-resistant colonies were isolated and maintained in medium supplemented with 5 μg/ml puromycin (Sigma-Aldrich).
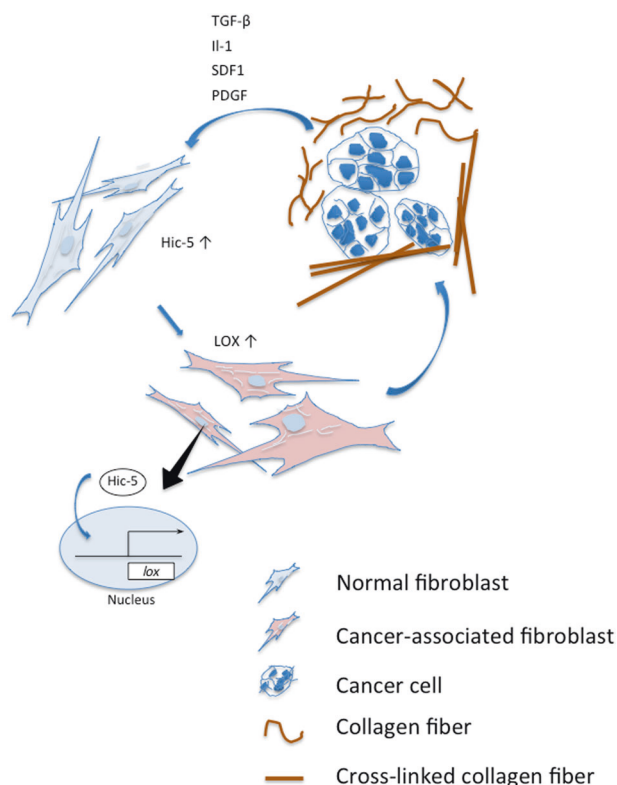

Fig. 8 Schematic model for Hic-5 contribution to the development of colorectal cancer attributed to ECM remodeling. Cancer-related cytokines such as TGF-β, PDGF, IL-1β and SDF-1 induced Hic-5 in NFs, and NFs acquired CAF phenotype. Concurrently Hic-5 accumulated in the nucleus of NFs and that induced LOX expression. LOX catalyze the covalent cross-linking of collagen fibers that increase ECM stiffness, and augment tumor progression

Cell culture

Caco-2, human NFs and CAFs were cultured in DMEM supplemented with 10% FBS and 1% penicillin/streptomycin. Primary cells used in experiments had been passaged less than 6 times. For fibroblast activation (Figs. 4c,e, f), NFs were grown to subconfluence and serum starved for 24 h, then treated for 24 h with 10 ng/mL TGF-β1 (R&D SYSTEMS), IL-1β (PEPROTECH), PDGF (WAKO Chemicals), SDF-1α (PEPROTECH) and freshly prepared conditioned media (CM) that was obtained by 48 h serum-starved cells, clarified by centrifugation. Caco-2, a human colon cancer cell line, and human colonic epithelial cells (HCoEpiC) were purchased from the RIKEN BioResource Center (RCB0988, Tsukuba, Japan; 2014) and ScienCell Research Laboratories (#2950), respectively. After receiving, the cells were expanded at early passages, and stocked in liquid nitrogen. The newly stocked vials were used in each experiment within passages for up to 2 months. This cell line was authenticated by the RIKEN BioResource Center by isoenzyme analysis, karyotype analysis and STR profiles.

Immunohistochemistry for human and mouse colon sections

Five μm sections of paraffin-embedded human and mouse colon tissues were used. For immunohistochemistry, anti-Hic-5 antibody (BD, #611164,1:100) was used as a primary antibody, followed by incubation with horseradish peroxidase (HRP)-conjugated goat anti-mouse IgG (DAKO). Immunoreactions were visualized using 3,3'-diaminobenzidine (DAB; DAKO) as a substrate in human tissues.

For immunofluorescence, sections were stained overnight with the antibodies against Hic-5 (BD, #611164, 1:100), CD31 (BD, #553370, 1:100), CD45 (BD, #550539, 1:100), Iba1 (Wako, #016-26721, 1:100) and α-SMA (Abcam, #ab5694, 1:100) at 4 °C. Sections were then incubated with fluorochrome-conjugated secondary antibodies (Alexa 488 or 568, Invitrogen. 1:1000) for 30 mins. Only in mouse tissues, a FITC-conjugated anti-α-SMA antibody (Sigma-Aldrich, #F3777, 1:100) was applied and incubated for 2 h at room temperature. Diaminophenylindole (DAPI) was used for nucleus staining. Each section was stained with hematoxylin and eosin (H&E) as a control.

Immunocytochemistry for NFs and CAFs extracted from human tissues

Cultured primary NFs and CAFs, or co-cultures with Caco-2 were fixed in 10% buffered formalin for 15 min at room temperature and washed with PBS-T (PBS containing 0.1% Tween-20) thrice. Cells were blocked with Protein Block (DAKO) for 20 min and incubated with anti-Hic-5 antibody (BD, #611164, 1:100), anti-LOX (Abcam, #ab31238, 1:100), anti-Collagen I (Abcam, #ab34710, 1:100) and anti-E-cadherin (BD, #61081, 1:100) antibodies at 4 °C overnight. After washing with PBS-T, cells were incubated with a fluorochrome-conjugated secondary antibody (Alexa 488 or 568, Invitrogen. 1:1000) for 30 min. DAPI was used for nucleus staining.

Assessment of the fraction of stromal cells in tumor tissue

We downloaded publicly available gene expression data of colon cancer from GEO (https://www.ncbi.nlm.nih.gov/geo/) or FIREBROWSE (http://firebrowse.org). The data processing was performed in an appropriate manner as described previously [33]. As a reference to the previous reports [34, 35], we used GSE14333, GSE33113, GSE39582, and TCGA COADREAD data sets to investigate an association of the expression of TGFB1I1 gene (coding for Hic-5) with the fraction of stromal cells in tumor tissue. To assess the fraction of stromal cells in tumor tissue, we calculated the stromal score based on ESTIMATE

algorithm [33]. To confirm higher TGFB1I1 expression in stromal cells compared to epithelial cells in colon cancer, we also used the GSE35602 and GSE39395 data sets, which include gene expression data of epithelium and stroma isolated from colon cancer tissue using laser-micro dissection or flow cytometry.

Western blot analysis

Western blot analysis was performed as described previously [10]. Briefly, we used primary antibody against LOX (Abcam, #Ab31238), α-SMA (Sigma-Aldrich, #A2547), Hic-5 (BD, #611164), HA tag (Gene Tex, #GTX115044) or GAPDH (Millipore, #AB2302). Positive bands were visualized with a horseradish peroxidase-conjugated second antibody and Western Lightning chemiluminescence reagent (PerkinElmer), followed by exposure to X-ray film (RX-U; Fuji Film Co). The densities of the bands were measured using the Densitograph software (AE-6962FC, CS Analyzer ver2.0; ATTO).

Real-time reverse transcriptase polymerase chain reaction

Total RNA was obtained from human colon tissues or cultured cells using the Trizol Reagent (Invitrogen). Real-time PCR was performed to quantify the expression of several genes in cultured cells and liver tissues using an ABI7900 real-time PCR detection system (Applied Bio systems, Foster City, CA, USA). Tests were run in quadruplicate and results averaged. Each value was adjusted using housekeeping gene (GAPDH) levels as reference, and fold-changes were calculated with respect to the control group using the $2^{-\Delta\Delta}$ Ct. Primer sequences used are follows: TGFβ1I1 (*HIC-5*); 5'-AGTGCTACTTTGAGCGCTTCTC-3' (forward), 5'-GCCGAAGAGCTTCAGGAAGCAAGG-3' (reserve), Collagen I (*COL1A1*); 5'-CCCGGGTTTCA-GAGACAACTTC-3' (forward), 5'-TCCA-CATGCTTTATTCCAGCAATC-3' (reserve), GAPDH (*GAPDH*); 5'-GCACCGTCAAGGCTGAGAAC-3' (forward), 5'-TGGTGAAGACGCCAGTGGA-3' (reserve).

Plasmid construction and transfection

pHM6/hic-5 (−NLS-Hic-5 in Fig. 6) was constructed by inserting the PCR-amplified cDNA fragment containing the full-length mouse *hic-5* into pHM6 vector harboring HA sequence. For the nuclear targeted version of Hic-5, pHM6/+NLS-hic-5 (+NLS-Hic-5 in Fig. 6), the synthesized nuclear localization signal (NLS) from SV40 large T antigen was inserted into pHM6/hic-5 vector to express the fusion proteins carrying NLS between N-terminals HA-tag and hic-5. The expression vectors were introduced into NFs

by Nucleofector system (4D-Nucleofector™ Lonza), and the cells were processed for analysis 72 h after transfection.

Adenovirus infection

To restore the expression of Hic-5, human primary NFs were infected for 48 h with a recombinant adenovirus encoding Hic-5 or β-galactosidase as a control.

Co-culture assay

To further examine the influence of direct contact with fibroblasts, we constructed a direct contact co-culture model. NFs (wild-type or shHic-5) were seeded confluently on the 10 cm plate, then Caco-2 cells were seeded at a density of 1.0×10^5 cells/ml and incubated with 10% FBS medium. After 24 h, we changed 10% FBS medium to FBS free medium. Then we measured long-axis (A) and short-axis (B) diameters of Caco-2 colony and calculated the areas ($S = AB\pi/4$) at two time points.

AOM-induced colon carcinogenesis model

All experiments were conducted in accordance with the protocols approved by the Institutional Committee for Animal Research of Showa University. All of the mice were bred in C56BL/6 background genotype. Pathogen-free 8 to 12 week-old male WT and Hic-5 deficient mice were injected intraperitoneally with 12.5 mg/kg body weight of AOM dissolved in physiological saline once a week for 6 weeks. Nine and 14 weeks thereafter, the animals were sacrificed for macroscopical inspection and histological analysis.

Statistical analysis

Animals were randomly allocated to control and treatment groups. Experiments were not performed blinded. Sample size was chosen to verify satisfactory inter-animal reproducibility. All the recorded data included the means ± SEM of the replicate samples ($n = 3$ to 6, depending on the experiment) and experiments were repeated a minimum of three times. Differences between two groups were assessed using a Mann–Whitney test (Figs. 1,4,5,6 and 7) and a Fisher's exact test (Table 1). Differences were considered statistically significant at a p value of <0.05.

Compliance with ethical standards

References

1. Levental I, Levental KR, Klein EA, Assoian R, Miller RT, Wells RG, et al. A simple indentation device for measuring micrometer-scale tissue stiffness. J Phys Condens Matter 2010;22:194120.
2. Cox TR, Erler JT. Remodeling and homeostasis of the extracellular matrix: implications for fibrotic diseases and cancer. Dis Model Mech 2011;4:165–78.
3. Bissell MJ, Radisky D. Putting tumours in context. Nat Rev Cancer 2001;1:46–54.
4. Csiszar K. Lysyl oxidases: a novel multifunctional amine oxidase family. Prog Nucleic Acid Res Mol Biol 2001;70:1–32.
5. Kagan HM, Li W. Lysyl oxidase: properties, specificity, and biological roles inside and outside of the cell. J Cell Biochem 2003;88:660–72.
6. Cox TR, Rumney RM, Schoof EM, Perryman L, Hoye AM, Agrawal A, et al. The hypoxic cancer secretome induces pre-metastatic bone lesions through lysyl oxidase. Nature 2015;522:106–10.
7. Baker AM, Bird D, Lang G, Cox TR, Erler JT. Lysyl oxidase enzymatic function increases stiffness to drive colorectal cancer progression through FAK. Oncogene 2013;32:1863–8.
8. Levental KR, Yu H, Kass L, Lakins JN, Egeblad M, Erler JT, et al. Matrix crosslinking forces tumor progression by enhancing integrin signaling. Cell 2009;139:891–906.
9. Shibanuma M, Kim-Kaneyama JR, Ishino K, Sakamoto N, Hishiki T, Yamaguchi K, et al. Hic-5 communicates between focal adhesions and the nucleus through oxidant-sensitive nuclear export signal. Mol Biol Cell 2003;14:1158–71.
10. Lei XF, Fu W, Kim-Kaneyama JR, Omoto T, Miyazaki T, Li B, et al. Hic-5 deficiency attenuates the activation of hepatic stellate cells and liver fibrosis through upregulation of Smad7 in mice. J Hepatol 2016;64:110–7.
11. Arita-Okubo S, Kim-Kaneyama JR, Lei XF, Fu WG, Ohnishi K, Takeya M, et al. Role of Hic-5 in the formation of microvilli-like structures and the monocyte-endothelial interaction that accelerates atherosclerosis. Cardiovasc Res 2015;105:361–71.
12. Lei XF, Kim-Kaneyama JR, Arita-Okubo S, Offermanns S, Itabe H, Miyazaki T, et al. Identification of Hic-5 as a novel scaffold for the MKK4/p54 JNK pathway in the development of abdominal aortic aneurysms. J Am Heart Assoc 2014;3:e000747.
13. Jamba A, Kondo S, Urushihara M, Nagai T, Kim-Kaneyama JR, Miyazaki A, et al. Hydrogen peroxide-inducible clone-5 regulates mesangial cell proliferation in proliferative glomerulonephritis in mice. PLoS One 2015;10:e0122773.
14. Varney SD, Betts CB, Zheng R, Wu L, Hinz B, Zhou J, et al. Hic-5 is required for myofibroblast differentiation by regulating mechanically dependent MRTF-A nuclear accumulation. J Cell Sci 2016;129:774–87.
15. Solomon JD, Heitzer MD, Liu TT, Beumer JH, Parise RA, Normolle DP, et al. VDR activity is differentially affected by Hic-5 in prostate cancer and stromal cells. Mol Cancer Res 2014;12:1166–80.
16. Kim-Kaneyama JR, Takeda N, Sasai A, Miyazaki A, Sata M, Hirabayashi T, et al. Hic-5 deficiency enhances mechanosensitive

apoptosis and modulates vascular remodeling. J Mol Cell Cardiol 2011;50:77–86.

17. Fearon ER, Vogelstein B. A genetic model for colorectal tumorigenesis. Cell 1990;61:759–67.

18. Zhou L, Yang K, Andl T, Wickett RR, Zhang Y. Perspective of Targeting Cancer-Associated Fibroblasts in Melanoma. J Cancer 2015;6:717–26.

19. Vasudev NS, Reynolds AR. Anti-angiogenic therapy for cancer: current progress, unresolved questions and future directions. Angiogenesis 2014;17:471–94.

20. Kraman M, Bambrough PJ, Arnold JN, Roberts EW, Magiera L, Jones JO, et al. Suppression of antitumor immunity by stromal cells expressing fibroblast activation protein-alpha. Science 2010;330:827–30.

21. Orimo A, Gupta PB, Sgroi DC, Arenzana-Seisdedos F, Delaunay T, Naeem R, et al. Stromal fibroblasts present in invasive human breast carcinomas promote tumor growth and angiogenesis through elevated SDF-1/CXCL12 secretion. Cell 2005;121:335–48.

22. Takai K, Le A, Weaver VM, Werb Z. Targeting the cancer-associated fibroblasts as a treatment in triple-negative breast cancer. Oncotarget 2016;7:82889–901.

23. Allaoui R, Bergenfelz C, Mohlin S, Hagerling C, Salari K, Werb Z, et al. Cancer-associated fibroblast-secreted CXCL16 attracts monocytes to promote stroma activation in triple-negative breast cancers. Nat Commun 2016;7:13050.

24. Deakin NO, Turner CE. Distinct roles for paxillin and Hic-5 in regulating breast cancer cell morphology, invasion, and metastasis. Mol Biol Cell 2011;22:327–41.

25. Wu JR, Hu CT, You RI, Pan SM, Cheng CC, Lee MC, et al. Hydrogen peroxide inducible clone-5 mediates reactive oxygen species signaling for hepatocellular carcinoma progression. Oncotarget 2015;6:32526–44.

26. Shola DT, Wang H, Wahdan-Alaswad R, Danielpour D. Hic-5 controls BMP4 responses in prostate cancer cells through interacting with Smads 1, 5 and 8. Oncogene 2012;31:2480–90.

27. Drori S, Girnun GD, Tou L, Szwaya JD, Mueller E, Xia K, et al. Hic-5 regulates an epithelial program mediated by PPARgamma. Genes Dev 2005;19:362–75.

28. Goreczny GJ, Ouderkirk-Pecone JL, Olson EC, Krendel M, Turner CE. Hic-5 remodeling of the stromal matrix promotes breast tumor progression. Oncogene. 2017;36:2693–2703.

29. Bonnans C, Chou J, Werb Z. Remodelling the extracellular matrix in development and disease. Nat Rev Mol Cell Biol 2014;15:786–801.

30. Dabiri G, Tumbarello DA, Turner CE, Van de Water L. Hic-5 promotes the hypertrophic scar myofibroblast phenotype by regulating the TGF-beta1 autocrine loop. J Invest Dermatol 2008;128:2518–25.

31. Wang TH, Hsia SM, Shieh TM. Lysyl oxidase and the tumor microenvironment. Int J Mol Sci. 2016;18: pii: E62.

32. Voloshenyuk TG, Landesman ES, Khoutorova E, Hart AD, Gardner JD. Induction of cardiac fibroblast lysyl oxidase by TGF-beta1 requires PI3K/Akt, Smad3, and MAPK signaling. Cytokine 2011;55:90–97.

33. Yoshihara K, Shahmoradgoli M, Martinez E, Vegesna R, Kim H, Torres-Garcia W, et al. Inferring tumour purity and stromal and immune cell admixture from expression data. Nat Commun 2013;4:2612.

34. Calon A, Lonardo E, Berenguer-Llergo A, Espinet E, Hernando-Momblona X, Iglesias M, et al. Stromal gene expression defines poor-prognosis subtypes in colorectal cancer. Nat Genet 2015;47:320–9.

35. Isella C, Terrasi A, Bellomo SE, Petti C, Galatola G, Muratore A, et al. Stromal contribution to the colorectal cancer transcriptome. Nat Genet 2015;47:312–9.